AIP | Applied Physics Letters

Vertical conduction mechanism of the epitaxial graphene/n-type 4H-SiC heterojunction at cryogenic temperatures

M. J. Tadjer, T. J. Anderson, K. D. Hobart, L. O. Nyakiti, V. D. Wheeler et al.

Citation: Appl. Phys. Lett. **100**, 193506 (2012); doi: 10.1063/1.4712621
View online: http://dx.doi.org/10.1063/1.4712621
View Table of Contents: http://apl.aip.org/resource/1/APPLAB/v100/i19
Published by the American Institute of Physics.

Vertical conduction mechanism of the epitaxial graphene/n-type 4H-SiC heterojunction at cryogenic temperatures

M. J. Tadjer,[1,a)] T. J. Anderson,[2] K. D. Hobart,[2] L. O. Nyakiti,[2] V. D. Wheeler,[2] R. L. Myers-Ward,[2] D. K. Gaskill,[2] C. R. Eddy, Jr.,[2] F. J. Kub,[2] and F. Calle[3]
[1]*CEI Campus Moncloa, UPM-UCM, Madrid 28040, Spain*
[2]*Naval Research Laboratory, 4555 Overlook Ave., SW, Washington, DC 20375, USA*
[3]*Universidad Politécnica de Madrid, Madrid 28040, Spain*

(Received 4 March 2012; accepted 18 April 2012; published online 10 May 2012)

Vertical diodes of epitaxial graphene on n^- 4H-SiC were investigated. The graphene Raman spectra exhibited a higher intensity in the G-line than the 2D-line, indicative of a few-layer graphene film. Rectifying properties improved at low temperatures as the reverse leakage decreased over six orders of magnitude without freeze-out in either material. Carrier concentration of $\sim 10^{16}\,cm^{-3}$ in the SiC remained stable down to 15 K, while accumulation charge decreased and depletion width increased in forward bias. The low barrier height of 0.08 eV and absence of recombination-induced emission indicated majority carrier field emission as the dominant conduction mechanism. © *2012 American Institute of Physics*. [http://dx.doi.org/10.1063/1.4712621]

Single and multilayer graphene films have been the topic of abundant research for their unique properties as a two-dimensional material.[1] Among the many methods of producing graphene, such as mechanical exfoliation of highly oriented pyrolitic graphite (HOPG),[2] chemical vapor deposition (CVD) on transition metal surfaces,[3,4] Si sublimation from either Si- or C- face oriented SiC,[5,6] graphene oxide reduction,[7] and reduction of solid carbon sources,[8] among others, most graphene has needed a post-growth substrate transfer step. While graphene transfer technology has rapidly advanced, epitaxial graphene (EG) on SiC does not necessarily need such a step, and has been used in large-area integrated circuit fabrication.[9] Graphene-based transparent electrical contacts to semiconductor surfaces have been demonstrated as well.[10] Therefore, the vertical graphene/SiC heterojunction could be applied in a SiC-based device.

Depending on the metal used, the Fermi level could be engineered such that the graphene could be doped either n- or p-type, and the metal-graphene junction could be either unipolar or bipolar.[11] In a vertical structure, the substrate type has additional influence on the conduction properties. In past work, we have demonstrated excellent diode rectifying properties by growing nanocrystalline diamond (NCD) on epitaxial layers of 4H-SiC,[12,13] and most recently have discussed minority carrier injection based graphene/p-SiC vertical heterojunctions.[14] Here, we report on the vertical conduction properties of EG grown on n-type 4H-SiC, which is the material used in the contact area of n-channel SiC field-effect transistors.

An 18 μm thick SiC epitaxial layer with n-type conductivity ($N_D = 8 \times 10^{15}\,cm^{-3}$) was grown on a 4° towards $[1\bar{1}02]$ cut n^+ 4H-SiC substrate.[15] Epitaxial graphene was formed on this Si-face 4H-SiC epilayer using Si sublimation techniques described by Tedesco *et al.*[5] Specifically, the SiC surface was etched *in situ* for 5 min at 1520 °C under 80 slm (standard liters per minute) H_2 flow, followed by EG growth for 2 h at 1620 °C under 20 slm Ar flow, and a cooldown to 800 °C under 10 slm Ar flow. Device processing was performed using an etch-back process in order to avoid modifying the chemical and electrical properties of the graphene sheets by exposure to photoresist and organic solvents.[14] Therefore, e-beam evaporation of 20/100 nm thick Ti/Al with the Ti contacting the EG was performed first. The Ti layer improved Al adhesion to the graphene surface, and the Al layer ensured the graphene was electron-populated due to the negative Fermi level difference between the Al and graphene work functions.[16] The metal contacts were processed with an etch-back recipe (no lift-off) and developer-only photoresist removal. Vertical diode structures were formed with a six-step process: (1) resist patterning of the blanket metal coated samples to form a metal mask for mesa etching, (2) Al etching with a Transene Al Etch Type A, then Ti etching with a buffered oxide etchant dip, (3) graphene mesa etching in O_2 plasma, (4) second resist pattern of the metal layers, (5) second Al and Ti metal etch to form contacts, and (6) back-side SiC substrate metallization with a 300 nm thick blanket Al film, without any contact annealing. Figure 1(a) shows the fabricated vertical diode structures.

Electrical measurements were performed from the top-side to the back-site metal contacts, with the exception of the Hall and sheet/contact resistance measurements, measured using Van der Pauw (VDP) and linear transfer length method (LTLM) structures. The electrical measurements were performed using an Agilent 4156c parameter analyzer connected to a Janis LHe-cooled probe station. Raman spectroscopy was performed in a WITec confocal Raman setup with a 532 nm excitation line, 50 μm diameter collection fiber, 0.9 numerical aperture, and a 360 nm spot size. The collection volume was about 0.12 μm^3 for the approximately 1 μm depth resolution of the instrument.

An edge region of a graphene mesa (Fig. 1(b)) was mapped using the confocal Raman spectroscopy setup described above. Figure 2(a) shows the Raman intensity map of the G-line, and Fig. 2(b) shows the relative Raman shift of the G-line from the same area. Spectra from the edge

a)Author to whom correspondence should be addressed. Electronic mail: mtadjer@die.upm.es. Telephone: +34-666-592-375.

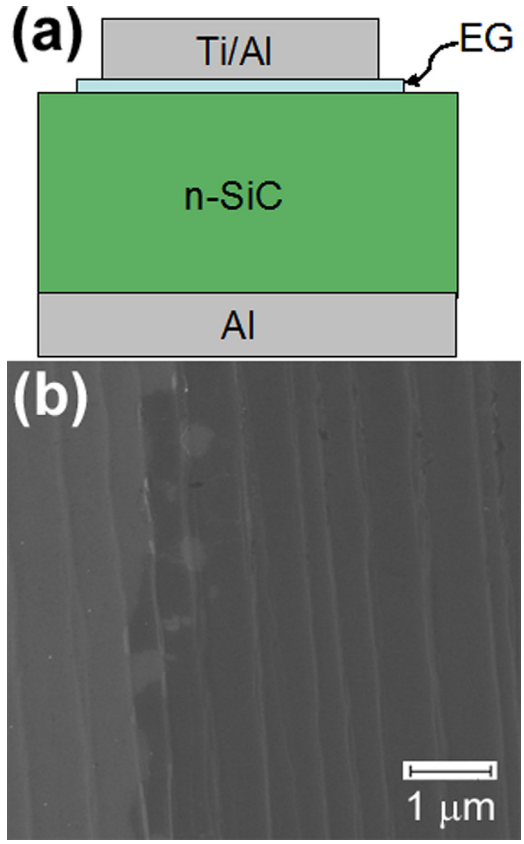

FIG. 1. (a) Schematic depiction of the EG/SiC vertical heterojunctions. (b) Scanning electron micrograph (5000× magnification, 5 kV beam field) of the stepped SiC surface with (right) and without (left) epitaxial graphene film.

(spectrum 2) and center of the graphene mesa (spectra 3 and 4) are given in Fig. 1(c), and compared with a spectrum from a region without graphene (spectrum 1). The defect-associated D-line was observed in spectrum 2 only, where the EG may have been partially etched by the O_2 plasma. The splitting of the G-line and the shift of the 2D line to a smaller wavenumber indicated layer nonuniformity around the etched EG edges.[17] The colors on both maps suggested good uniformity of the graphene away from the mesa edges. The greater intensity of the G-line with respect to the 2D line is usually indicative of few-layer graphene when on-axis SiC substrates are used.[4] A SiC substrate with a higher degree of miscut, and thus higher steps, will result in thicker EG compared to growth under identical conditions on SiC with a lower degree of miscut. From Fig. 1(b), we calculated 24-35 nm step heights for 4° miscut from the distance between terraces. The contrast between the graphene-covered area (right) and the n-type SiC surface (left), as well as small wrinkles in the EG near the step edges, qualitatively suggests the presence of 2-3 layers of EG Dimitrakopoulos *et al*. have reported 1-2 layers of EG on Si-face SiC with terraces' spacing comparable to that in our samples, and a minor effect of steps orientation with respect to current flow on the EG mobility.[18] Regardless of the precise number of EG layers, we emphasize that consistently stacked few-layer graphene will not have an energy gap and vertical conduction would be determined solely by electron transport into the SiC through the buffer layer.

Vertically measured current-voltage characteristics as a function of temperature are presented in Fig. 3(a). Even

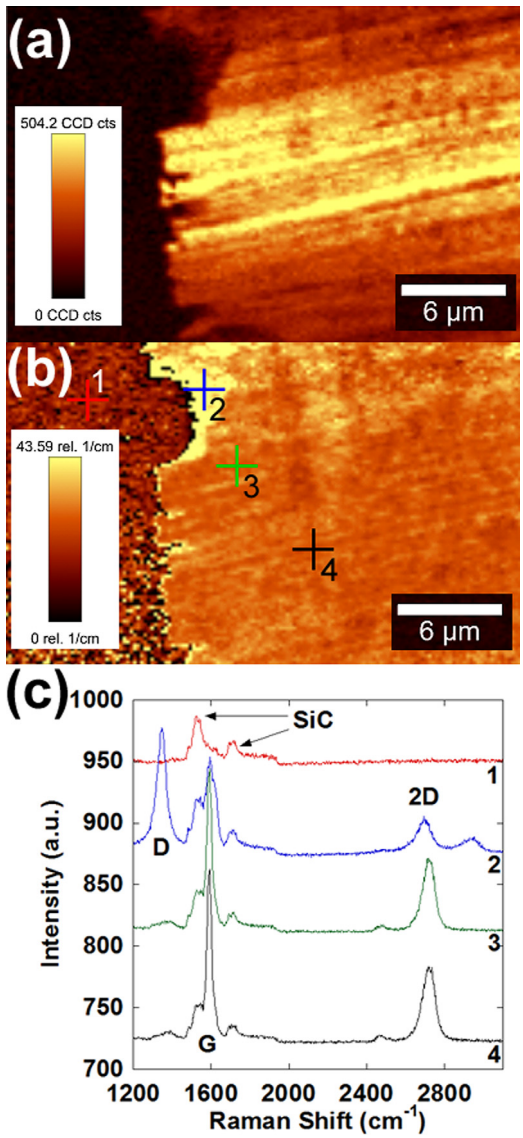

FIG. 2. Raman map of a graphene mesa edge: (a) intensity and (b) Raman shift of the G-line. Four points were chosen in (b) and the corresponding spectra are shown in (c): 1—off-graphene Raman spectrum showing only the secondary SiC peaks; 2—edge-graphene Raman spectrum showing the defect-related D-line; and 3 and 4—graphene Raman spectra from within the mesa structure.

though the current decreased at cryogenic temperatures in both forward and reverse biases, no evidence of carrier freezeout at low temperatures was observed. The sheet and contact resistances (R_{SH} and R_C) of the EG were measured on a LTLM test structure. R_{SH} increased from 1408 Ω/sq. at 300 K to 1706 Ω/sq. at 30 K, while R_C was maintained within the 3-7 $\times 10^{-6}$ Ω cm^2 range.

Using standard analysis techniques for metal-semiconductor contacts,[19,20] the forward-bias barrier height was extracted to be 0.08 eV from the Richardson plot in Fig. 3(b). Our hypothesis is that the image force caused by electrons in the graphene lowered the barrier height sufficiently to maximize tunneling probability into states close to the SiC conduction band edge. This mechanism, known as field emission, will have higher probability than electron tunneling into higher energy states (thermionic emission).[21] The model for barrier height extraction followed the Arrhenius behavior down to 140 K only. On the other hand, the

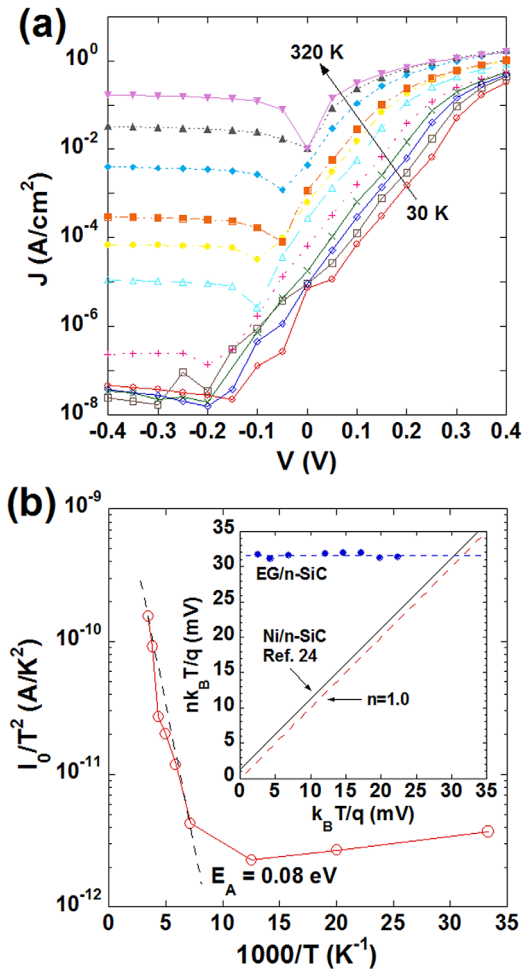

FIG. 3. (a) Temperature-dependent current-voltage (I-V-T) characteristics of the EG/n$^-$ SiC heterojunction from 30 K to 320 K in steps of 30 K. (b) Extraction of barrier height from the I-V-T data based on the observed linearity of the Arrhenius plot down to about 100 K. Inset: nk_BT/q-k_BT/q plot of EG/n$^-$ SiC and Ni/n$^-$ SiC from Ref. 24 indicating field vs. thermionic emission conduction mechanisms in each structure.

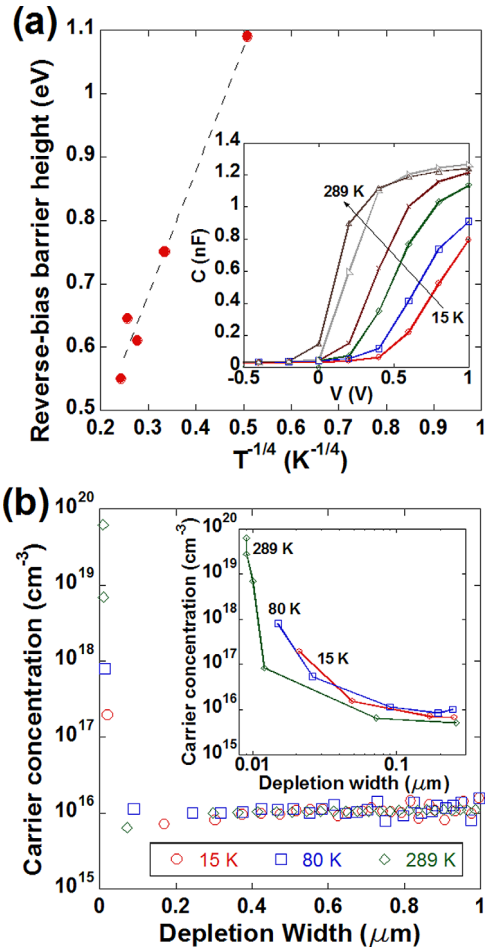

FIG. 4. (a) Temperature-dependent barrier height of the graphene/n-SiC heterojunction extracted from the $1/C^2$ intercept. Inset: temperature-dependent C-V characteristics. (b) Reverse-bias (depletion) carrier concentration as a function of temperature. Inset: carrier concentration and depletion width in forward bias (accumulation).

influence of the ideality factor, presented in the nk_BT/q-k_BT/q plot (Fig. 3(b) inset), resulted in nearly temperature-independent behavior ($nk_BT \cong 31$–32). This behavior has been shown to support field emission as the dominant conduction mechanism throughout the entire temperature range in classical metal-semiconductor interfaces.[22] In addition, Li *et al*. have demonstrated field emission at high temperatures in few-layer graphene dispersed on copper.[23] It should be noted that metallic contacts to 4H-SiC typically obey thermionic emission laws with a near-unity slope on a nk_BT/q-k_BT/q plot, as demonstrated by Roccaforte *et al*.[24] Therefore, in forward bias, the graphene acted as a temperature-independent charge-supply film causing field emission of electrons through the barrier layer into the SiC.

Independent capacitance-voltage analysis in reverse bias was carried out as well. The barrier height, extracted from the x-axis intercept of the $1/C^2$ curves and presented in Fig. 4(a), remained in the 0.55-0.75 eV range down to 80 K but increased sharply to 1.09 eV at 15 K. This result corroborated the barrier height temperature dependence observed below 80 K in forward bias. Typically, barrier height values are often lowered by defect-preferential conduction in a Schottky contact. Here, this could have occurred along the graphene mesa edges, where a D-line was observed.

The barrier height increase in reverse bias was correlated with the decrease in reverse current (Fig. 3(a)). The reverse bias current decreased more than six orders of magnitude in the 15-290 K measurement range. Considering that carrier donors in both EG and SiC remained active at low temperature, and that the depletion widened only by 0.08 μm (from 0.26 μm at RT to 0.35 μm at 15 K), the only major impediment for electron transfer from the EG to the SiC was the increased barrier height difference between the two layers. The linear increase in barrier height with $T^{-1/4}$ (Fig. 4(a)) suggested that the graphene film followed Mott's variable range hopping conductivity law.[25]

The capacitance-voltage analysis in Fig. 4(b) determined that the bulk carrier concentration of the 4H-SiC epilayer remained close to $1.05 \times 10^{16}\,cm^{-3}$ up to 1 μm depletion width in the 15-300 K range. However, the 1 V forward-bias electron concentration decreased from about $6 \times 10^{19}\,cm^{-3}$ at RT to $2 \times 10^{17}\,cm^{-3}$ at 15 K (Fig. 4(b) inset). Combined with the wider space charge region for low temperatures (9 nm at RT versus 21 nm at 15 K), it follows that less electrons will diffuse from the SiC into the EG sheets in forward bias. The heterojunction was identically biased under an

UV-IR spectrum sensitivity CCD to detect any possible emission from the junction. Unlike the EG/p-SiC junction in Ref. 14, no luminescence was observed, supporting the hypothesis that the EG/n-SiC heterojunction diode is a majority carrier device.

EG/n^- 4H-SiC heterojunctions have been investigated. The insertion of the graphene layer between the metal and SiC interface converted the conduction mechanism from thermionic emission to field-emission with a low defect-assisted forward bias barrier height. Comparable current levels in forward and reverse biases at room temperature converted to a Schottky-like conduction behavior at cryogenic temperatures. The reverse current decreased by over six orders of magnitude, resulting in much-improved rectifying properties at cryogenic temperatures. Absence of photon emission in forward bias indicated a majority carrier unipolar device. Integrated into an epitaxial SiC device process, such low turn-on voltage heterojunctions could offer an attractive contact solution.

The authors are indebted to Dr. Ute Schmidt of WITec for Raman spectroscopy and Dr. Joshua Caldwell of NRL for insightful discussions. Research by M. J. Tadjer has been partially supported by a PICATA postdoctoral fellowship of the Moncloa Campus of International Excellence, UCM-UPM. Partial support from projects RUE (CSD2009-00046) and AEGAN (TEC2009-14307), from Ministerio de Ciencia e Innovación of Spain, is also acknowledged. L. O. Nyakiti and V. D. Wheeler acknowledge support from the American Society for Engineering Education. Research at the U.S. Naval Research Laboratory was supported by ONR.

[1]A. H. Castro Neto, F. Guinea, N. M. R. Peres, K. S. Novoselov, and A. K. Geim, Rev. Mod. Phys. **81**, 109–162 (2009).
[2]A. Geim and A. H. MacDonald, Phys. Today **60**, 35 (2007).
[3]S. Bae, H. Kim, Y. Lee, X. Xu, J. S. Park, Y. Zheng, J. Balakrishnan, T. Lei, H. R. Kim, Y. I. Song, Y. J. Kim, K. S. Kim, B. Ozyilmaz, J. H. Ahn, B. H. Hong, and S. Iijima, Nat. Nanotechnol. **5**, 574 (2010).
[4]A. Reina, X. Jia, J. Ho, D. Nezich, H. Son, V. Bulovic, M. S. Dresselhaus, and J. Kong, Nano Lett. **9**(1), 30–35 (2009).
[5]J. L. Tedesco, B. L. VanMil, R. L. Myers-Ward, J. M. McCrate, S. A. Kitt, P. M. Campbell, G. G. Jernigan, J. C. Culbertson, C. R. Eddy, Jr., and D. K. Gaskill, Appl. Phys. Lett. **95**, 122102 (2009).
[6]P. Sutter, Nature Mater. **8**, 171 (2009).
[7]D. Li, M. B. Muller, S. Gilje, R. B. Kaner, and G. G. Wallace, Nat. Nanotechnol. **3**, 101 (2008).
[8]Z. Sun, Z. Yan, J. Yao, E. Beitler, Y. Zhu, and J. M. Tour, Nature **468**, 549–552 (2010).
[9]Y.-M. Lin, A. Valdes-Garcia, S.-J. Han, D. B. Farmer, I. Meric, Y. Sun, Y. Wu, C. Dimitrakopoulos, A. Grill, P. Avouris, and K. A. Jenkins, Science **332**, 1294 (2011).
[10]J. D. Caldwell, T. J. Anderson, J. C. Culbertson, G. G. Jernigan, K. D. Hobart, F. J. Kub, M. J. Tadjer, J. L. Tedesco, J. K. Hite, M. A. Mastro, R. L. Myers-Ward, C. R. Eddy, Jr., P. M. Campbell, and D. K. Gaskill, ACS Nano **4**(2), 1108 (2010).
[11]P. A. Khomyakov, A. A. Starikov, G. Brocks, and P. J. Kelly, Phys. Rev. B **82**, 115437 (2010).
[12]M. J. Tadjer, K. D. Hobart, J. D. Caldwell, J. E. Butler, K. X. Liu, C. R. Eddy, Jr., D. K. Gaskill, K. K. Lew, B. L. VanMil, R. L. Myers-Ward, M. G. Ancona, F. J. Kub, and T. I. Feygelson, Appl. Phys. Lett. **91**, 163508 (2007).
[13]M. J. Tadjer, T. I. Feygelson, K. D. Hobart, J. D. Caldwell, T. J. Anderson, J. E. Butler, C. R. Eddy, Jr., D. K. Gaskill, K. K. Lew, B. L. VanMil, R. L. Myers-Ward, and F. J. Kub, Appl. Phys. Lett. **97**, 193510 (2010).
[14]T. J. Anderson, K. D. Hobart, L. O. Nyakiti, V. D. Wheeler, R. L. Myers-Ward, J. D. Caldwell, F. J. Bezares, D. K. Gaskill, C. R. Eddy, Jr., F. J. Kub, G. G. Jernigan, M. J. Tadjer, and E. A. Imhoff, "Investigation of the epitaxial graphene/p-SiC heterojunction" (unpublished).
[15]R. L. Myers-Ward, B. L. VanMil, R. E. Stahlbush, S. L. Katz, J. M. McCrate, S. A. Kitt, C. R. Eddy, Jr., and D. K. Gaskill, Mater. Sci. Forum **615–617**, 105 (2009).
[16]G. Giovannetti, P. A. Khomyakov, G. Brocks, V. M. Karpan, J. van den Brink, and P. J. Kelly, Phys. Rev. Lett. **101**, 026803 (2008).
[17]J. Röhrl, M. Hundhausen, K. V. Emtsev, Th. Seyller, R. Graupner, and L. Ley, Appl. Phys. Lett. **92**, 201918 (2008).
[18]C. Dimitrakopoulos, Y.-M. Lin, A. Grill, D. B. Farmer, M. Freitag, Y. Sun, S.-J. Han, Z. Chen, K. A. Jenkins, Y. Zhu, Z. Liu, T. J. McArdle, J. A. Ott, R. Wisnieff, and P. Avouris, J. Vac. Sci. Technol. B **28**(5), 985 (2010).
[19]S. M. Sze, *Physics of Semiconductor Devices* (Wiley, New York, 1981), p. 285.
[20]A. N. Saxena, Surf. Sci. **13**, 151–171 (1969).
[21]F. A. Padovani and R. Stratton, Solid-State Electron. **9**, 695 (1966).
[22]R. T. Tung, Phys. Rev. B **45**(23), 45 (1992).
[23]J. Li, J. Chen, B. Shen, X. Yan, and Q. Xue, Appl. Phys. Lett. **99**, 163103 (2011).
[24]F. Roccaforte, F. La Via, V. Raineri, R. Pierobon, and E. Zanoni, J. Appl. Phys. **93**, 9137 (2003).
[25]C. Godet, J. Non-Cryst. Solids **299–302**, 333–338 (2002).